SLAC-PUB-11697

HADRONIC PHYSICS STUDIES AT BaBar*

Roberto Stroili

Università di Padova & INFN
Via Marzolo 8, 35131 Padova, Italy
for the BaBar Collaboration

(Received November 4, 2005)

A new resonance, $Y(4260)$ with a mass of $4259 \pm 8^{+2}_{-6}\,\mathrm{MeV}/c^2$ and $J^{\mathrm{PC}} = 1^{--}$, discovered by the BaBar experiment shows peculiar behavior in his decay mode. The Λ_c^+ baryon mass has been measured, using its decays to $\Lambda K^0_{\mathrm{S}} K^+$ and $\Sigma^0 K^0_{\mathrm{S}} K^+$, and its value is $2286.46 \pm 0.14\,\mathrm{MeV}/c^2$, the precision is greatly improved w.r.t. PDG value. Ξ_c^0 and Ω_c^0 decays and production have been studied with results greatly improved w.r.t. PDG.

PACS numbers: 13.66.Bc, 13.66.Jn, 14.20.Jn, 14.40.Lb

1. Introduction

The very high statistics available at B-factories give experiments the opportunity to discover new states and the possibility of precision studies on rare processes. The discovery of the new resonance $Y(4260)$, a $J^{\mathrm{PC}} = 1^{--}$ state with mass $4259 \pm 8^{+2}_{-6}\,\mathrm{MeV}/c^2$ and full width of $88 \pm 23^{+2}_{-6}\,\mathrm{MeV}/c^2$ is presented. This resonance shows a peculiar behavior as its main decay mode seems to be through $J/\psi\pi^+\pi^-$ that would exclude the possibility for the $Y(4260)$ of being a $c\bar{c}$ radial excitation state. Λ_c^+ mass is measured with precision greatly improved w.r.t. PDG value through its low Q-value[1] (and low branching ratio) decay modes $\Lambda_c^+ \to \Lambda K^0_{\mathrm{S}} K^+$ and $\Lambda_c^+ \to \Sigma^0 K^0_{\mathrm{S}} K^+$. Charmed baryon Ω_c^0 and Ξ_c^0 production modes are studied together with the decays Ω_c^0 to $\Omega^-\pi^+$, $\Omega^-\pi^+\pi^-\pi^+$, $\Xi^- K^-\pi^+\pi^+$ and Ξ_c^0 to $\Omega^-\,K^+$ and $\Xi^-\,\pi^+$.

* Presented at the XXIX International Conference of Theoretical Physics, "Matter to the Deepest", Ustroń, Poland, September 8–14, 2005.

[1] For a decay mode $A \to BC$ the Q-value is defined as $Q = m_A - m_B - m_C$.

Contributed to 29th International Conference of Theoretical Physics: Matter to the Deepest: Recent Developments in Physics of Fundamental Interactions, Ustron, Poland, 8-14 September 2005

Work supported in part by Department of Energy contract DE-AC02-76SF00515

2. The BaBar detector

The BaBar detector, a general-purpose, solenoidal, magnetic spectrometer, is described in detail elsewhere [1]. Charged-particle momenta are measured in a tracking system consisting of a five-layer double-sided silicon vertex tracker (SVT) and a 40-layer central drift chamber (DCH), both situated in a 1.5 T axial magnetic field. The transverse momentum resolution is $\sigma_{p_t}/p_t = (0.13 \pm 0.01)\% \times p_t \oplus (0.45 \pm 0.03)\%$, where p_t is measured in GeV. A ring-imaging Cherenkov detector (DIRC) is used for charged-particle identification. Photons are detected and measured with a CsI electromagnetic calorimeter (EMC). Electron candidates are identified by the ratio of the shower energy deposited in the EMC to the momentum, shower shape, specific ionization in the DCH, and Cherenkov angle measured by the DIRC. Photons candidates are clusters in the EMC that have a shape consistent with an electromagnetic shower but without an associated charged track. Muons candidates are selected based on a likelihood formed from penetration, and shower shape in the IFR, plus IFR and DCH tracking. Kaon and proton particle identification is performed with dE/dx and Cherenkov angle measurements.

3. $Y(4260)$

Recent experiments have reported an unexpectedly narrow state, the $X(3872)$ was observed through its decay to $\pi^+\pi^- J/\psi$ [2]. The $X(3872)$ has not been observed in e^+e^- annihilations with initial state radiation (ISR) [3] at 10.6 GeV [4], but this search in the decay channel $\pi^+\pi^- J/\psi$ showed an enhancement in the invariant mass distribution at an energy of about 4260 MeV. This analysis [5] has been done using data from an integrated luminosity of 210.55 fb^{-1} collected at $\sqrt{s} = 10.58$ GeV near the peak of the $\Upsilon(4S)$ meson (*on resonance*) plus 21.60 fb^{-1} collected approximately 40 MeV below this energy (*off resonance*).

Candidate J/ψ mesons are reconstructed via their decays to e^+e^- and $\mu^+\mu^-$. The lepton tracks must be well reconstructed, and at least one must be identified as an electron or a muon. The J/ψ candidate is combined with a pair of oppositely charged tracks that are identified as pions.

The mass region from 4.2 to 4.4 GeV/c^2 is excluded from consideration in the optimization of the selection criteria with the full sample to avoid the introduction of statistical or other biases in the analysis of this region. Radiative production of the $\psi(2S)$ is used as a clean benchmark process [6] for a data-driven optimization. Simulated ISR events are validated with the $\psi(2S)$ data and are used to extrapolate the selection criteria to the excluded mass region as appropriate for small kinematic differences due to the higher mass.

The radiative $e^+e^- \to \gamma_{\rm ISR}(\pi^+\pi^- J/\psi)$ events are characterized by a small recoil mass against the $\pi^+\pi^- J/\psi$ system, and low missing transverse momentum. The final selection criteria reflect these properties: (1) no additional well-reconstructed charged tracks, (2) the transverse component of the missing momentum in the e^+e^- center of mass frame must be less than 2.5 GeV, (3) the mass recoiling against the $\pi^+\pi^- J/\psi$ combination must be within $[-1.012, +1.807]\,{\rm GeV}/c^2$ for e^+e^- and $[-1.029, +1.119]\,{\rm GeV}/c^2$ for $\mu^+\mu^-$, respectively, (4) the lepton helicity, $\theta_{\rm h}(J/\psi)$ satisfies $|\cos\theta_{\rm h}(J/\psi)| < 0.90$, and (5) for the e^+e^- mode, $\cos\theta_{\pi^+} < 0.90$ is required to reject a forward peaking background, where θ_{π^+} is the angle between the π^+ momentum in the $\pi^+\pi^-$ rest frame and the $\pi^+\pi^-$ momentum in the $\pi^+\pi^- J/\psi$ rest frame. For $\gamma_{\rm ISR}\psi(2S)$ events, the θ_{π^+} distribution is flat.

Candidate $\pi^+\pi^-\ell^+\ell^-$ tracks are refit with a common vertex, and the lepton pair is kinematically constrained to the J/ψ mass. The resulting $\pi^+\pi^- J/\psi$ mass resolution function is well-described by a Cauchy distribution with a width of $4.2\,{\rm MeV}/c^2$ for the $\psi(2S)$ and $5.3\,{\rm MeV}/c^2$ at $4.3\,{\rm GeV}/c^2$.

The $\pi^+\pi^- J/\psi$ invariant mass spectrum from 3.8 to $5.0\,{\rm GeV}/c^2$ is shown Fig. 1(a); an enhancement just above $4.25\,{\rm GeV}/c^2$ is clearly observed; the figure inset includes the $\psi(2S)$ region for comparison. An unbinned likelihood fit to the $\pi^+\pi^- J/\psi$ mass spectrum using a Breit–Wigner signal function convoluted with a $5.3\,{\rm MeV}/c^2$-wide Cauchy resolution function and a 2nd order polynomial yields 127±24 events, with a mass of $4259 \pm 8\,{\rm MeV}/c^2$ and a width of $88 \pm 23\,{\rm MeV}/c^2$. The statistical significance of 8.2σ is determined from $\sqrt{-2\ln(\mathcal{L}_0/\mathcal{L}_{\rm max})}$, where $\mathcal{L}_{\rm max}$ is the likelihood of the fit shown in Fig. 1(a), and $\mathcal{L}_0$ is a null signal fit to the same data.

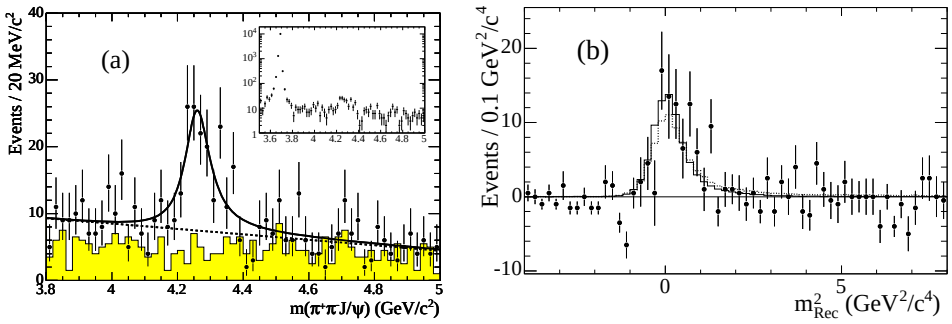

Fig. 1. (a) $\pi^+\pi^- J/\psi$ invariant mass spectrum, the points with error bars represent the data and the shaded histogram represents the background. The solid curve shows the result of the single-resonance fit; the dashed curve represents the background component. (b) $m^2_{\rm Rec}$ distribution, the points with error bars represent the data, the solid line is from $Y(4260)$ ISR MC and the dashed line the $\psi(2S)$ data.

The robustness of the $Y(4260)$ signal is studied splitting the data samples according to various criteria (J/ψ decay modes, acquisition periods, with and without $\gamma_{\rm ISR}$) together with the control sample, all the fits of these subsamples give consistent results.

It is important to demonstrate the ISR production mechanism as the $J^{\rm PC} = 1^{--}$ assignment for the $Y(4260)$ follows. The ISR photon is reconstructed in (24±8)% of $Y(4260)$ events, in excellent agreement with the 25% observed for ISR $\psi(2S)$. Various kinematic distributions for the signal have been studied. The distribution of $m^2_{\rm Rec}$ is shown in Fig. 1(b), along with corresponding distributions for ISR $\psi(2S)$ data events and for ISR $Y(4260)$ Monte Carlo events. Good agreement is found for these distributions, and for all other quantities studied to test that initial-state radiation is responsible for these events.

When the systematic uncertainties are included, the $Y(4260)$ mass is determined to be $4259 \pm 8({\rm stat})^{+2}_{-6}({\rm syst})$ MeV/c^2 and width $88 \pm 23({\rm stat})$ $^{+6}_{-4}({\rm syst})\,{\rm MeV}/c^2$.

The production cross section times branching fraction of the $Y(4260)$ $\Gamma_{ee}(Y)\,\mathcal{B}(Y \to \pi^+\pi^- J/\psi)$ is determined to be $5.5 \pm 1.1^{+0.8}_{-0.7}\,{\rm eV}$, where the second error is systematic arising from uncertainties due to fit procedure and selection, errors on Γ_{ee} of the $\psi(2S)$ and $\mathcal{B}(\psi(2S) \to \pi^+\pi^- J/\psi)$.

No enhancement has been observed in the cross section for $e^+e^- \to$ hadrons [7] at energies corresponding to the $Y(4260)$. We compute the cross section for $e^+e^- \to \pi^+\pi^- J/\psi$ production at 4.25 GeV, corresponding to the highest bin in our data, to be about 50 pb. The inclusive hadronic cross section at $\sqrt{s} = 4.25\,{\rm GeV}$ is 14.2 nb [7]. The ratio, approximately 0.34%, is smaller than the 4% experimental uncertainty for the hadronic cross section, so this mode would not have been visible. However, if the branching fraction of $Y(4260)$ to $\pi^+\pi^- J/\psi$ is very small, decays to other hadronic modes like $D\overline{D}$ would have been observable, this indicates that the branching fraction to $\pi^+\pi^- J/\psi$ must be large compared to that for $\psi(3770)$.

At the current level of statistics it is not possible to distinguish the number of new states; the data can be characterized by a single resonance of mass $\sim 4.26\,{\rm GeV}/c^2$ and of width $\sim 90\,{\rm MeV}/c^2$. It is puzzling that a broad and heavy resonance like $Y(4260)$ would decay visibly to $\pi^+\pi^- J/\psi$. If enhanced $\pi^+\pi^- J/\psi$ decays are indicative of a new class of $c\overline{c}$ states, then perhaps there is a relationship with the equally intriguing $X(3872)$ state.

4. Λ_c^+ mass measurement

The data sample used for the Λ_c^+ mass measurement [8] comprises an integrated luminosity of 232 fb^{-1} collected on and off resonance. The Λ_c^+ decay modes studied are $\Lambda\, K^0_{\rm S}\, K^+$ and $\Sigma^0\, K^0_{\rm S}\, K^+$, despite their low branch-

ing fraction, the reduced Q-value of this reaction gives a reduced systematic uncertainty that over-compensates the loss in statistical precision.

The $\Lambda_c^+ \to \Lambda K_S^0 K^+$ signal is reconstructed using only the charged two-body decay modes of the Λ and K_S^0 hadrons: $\Lambda \to p\pi^-$ and $K_S^0 \to \pi^+\pi^-$; the tracks are fitted to a common vertex constraining the masses to the PDG values. The Λ and K_S^0 candidates are then combined with a fifth track, identified as a charged kaon, in a fit to a common vertex to form a Λ_c^+ candidate. To suppress background, which results mainly from B decays, the momentum (p^*) of the Λ_c^+ candidate in the e^+e^- center-of-mass frame (CM) is required to be at least $2\,\mathrm{GeV}/c$. This requirement also helps to reduce systematic uncertainties that affect mainly low-momentum tracks. The selection efficiency, not including branching fractions, is about 15% for $\Lambda_c^+ \to \Lambda K_S^0 K^+$ decays with Λ_c^+ CM momentum larger than $2\,\mathrm{GeV}/c$. The background is suppressed sufficiently not to be an issue for the Λ_c^+ mass measurement.

The $\Lambda_c^+ \to \Sigma^0 K_S^0 K^+$ mode is reconstructed from $\Sigma^0 \to \Lambda\gamma$ and Λ and K_S^0 hadrons decaying into two charged particles. The Λ and K_S^0 candidates are formed in the same way as in the $\Lambda_c^+ \to \Lambda K_S^0 K^+$ selection. A Σ^0 candidate is formed by combining a Λ candidate with a photon. The Σ^0 candidates are fit with their mass constrained to the PDG mass and are combined with K_S^0 and K^+ candidates to form Λ_c^+ candidates that must satisfy the same invariant mass, vertex probability, and p^* requirements as $\Lambda_c^+ \to \Lambda K_S^0 K^+$ candidates. The selection efficiency, not including branching fractions, is estimated to be about 8% for $\Lambda_c^+ \to \Sigma^0 K_S^0 K^+$ decays with Λ_c^+ CM momentum larger than $2\,\mathrm{GeV}/c$.

The decay modes $\Lambda_c^+ \to pK^-\pi^+$ and $\Lambda_c^+ \to pK_S^0$ are used for cross checks, their signal-selection efficiency is, respectively, about 42% and 41% and depends on the Λ_c^+ momentum. For the cross check studies also the large samples of Λ and K_S^0 decays are reconstructed using similar criteria as those used to select Λ and K_S^0 candidates for $\Lambda_c^+ \to \Lambda K_S^0 K^+$ decays. The mass-constrained vertex fits are replaced with geometric vertex fits.

The invariant mass distribution for the $\Lambda_c^+ \to \Lambda K_S^0 K^+$ candidates is shown in Fig. 2(a). A clear Λ_c^+ signal peak is observed. A binned maximum likelihood fit to the mass distribution is performed using a sum of two Gaussians with a common mean for the Λ_c^+ signal function. The background is described by a linear function as suggested by simulation studies. The fit parameter values are given in Table I. Note that the uncertainty on the mean mass is statistical only. The invariant mass distribution for the $\Lambda_c^+ \to \Sigma^0 K_S^0 K^+$ candidates is shown in Fig. 2(b). A small but significant Λ_c^+ signal peak is observed. The figure also shows the expected background under the Λ_c^+ peak from $\Lambda_c^+ \to \Sigma^0 K_S^0 K^+$ decays with a correct Λ but a wrong photon used in candidate selection. A binned maximum likelihood

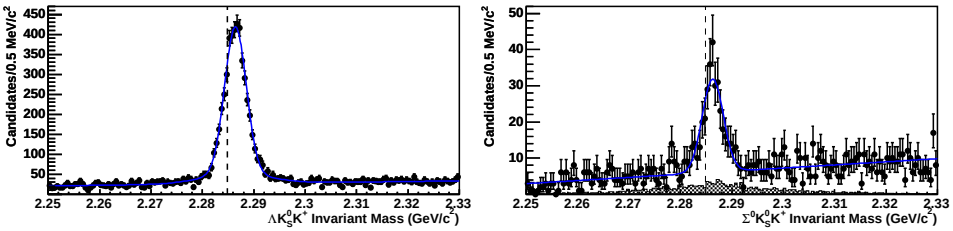

Fig. 2. Invariant mass distributions for (a) $\Lambda_c^+ \to \Lambda K_S^0 K^+$, (b) $\Lambda_c^+ \to \Sigma^0 K_S^0 K^+$, the dashed line shows the present PDG value.

fit of the mass distribution is performed using a single Gaussian for the Λ_c^+ signal. The background is described by a linear function. The wrongly-reconstructed $\Lambda_c^+ \to \Sigma^0 K_S^0 K^+$ candidates are absorbed into the signal and background because they peak at the Λ_c^+ mass. The fit parameter values are given in Table I.

TABLE I

Uncorrected fit mass values for the $\Lambda_c^+ \to \Lambda K_S^0 K^+$ and $\Lambda_c^+ \to \Sigma^0 K_S^0 K^+$ signals together with the half-width at half-maximum (HWHM) calculated from these values.

Parameter	$\Lambda_c^+ \to \Lambda K_S^0 K^+$	$\Lambda_c^+ \to \Sigma^0 K_S^0 K^+$
Fitted mass (MeV/c^2)	2286.44±0.04	2286.29±0.18
Signal yield (events)	4627±84	264±20
HWHM (MeV/c^2)	2.55±0.06	2.41±0.22

The invariant-mass distributions for the four control modes are studied; the fit yields, mass, and signal RMS values are listed in Table II. The fitted mass values for the Λ and K_S^0 are significantly below the PDG values. This disagreement has been studied in detail and is mainly due to an underestimation of the energy loss in the detector material, other sources for systematics have been found in the magnetic field knowledge and in detector geometry. A correction to the detector material description has been applied, the Λ_c^+ masses after correction are

$$m(\Lambda_c^+)_{\Lambda K_S^0 K^+} = 2286.501 \pm 0.042(\text{stat}) \pm 0.144(\text{syst})\,\text{MeV}/c^2$$
$$m(\Lambda_c^+)_{\Sigma^0 K_S^0 K^+} = 2286.303 \pm 0.181(\text{stat}) \pm 0.126(\text{syst})\,\text{MeV}/c^2\,.$$

The systematic uncertainties on the two measurements are highly, but not fully, correlated. The two mass measurements are combined using the BLUE (Best Linear Unbiased Estimate) technique [9], the result is

$$m(\Lambda_c^+) = 2286.46 \pm 0.14\,\text{MeV}/c^2\,.$$

TABLE II

Uncorrected values for the four decay modes used for cross-checks.

Parameter	$\Lambda \to p\pi^-$	$K^0_S \to \pi^+\pi^-$	$\Lambda_c^+ \to pK^-\pi^+$	$\Lambda_c^+ \to pK^0_S$
PDG mass (MeV/c^2)	1115.683 ± 0.006	497.648 ± 0.022	2284.900 ± 0.600	2284.900 ± 0.600
Fitted mass (MeV/c^2)	1115.660 ± 0.001	497.305 ± 0.002	2285.845 ± 0.013	2285.876 ± 0.023
Signal yield (events)	3192700 ± 5800	2463900 ± 4900	1449300 ± 5300	243700 ± 1900
HWHM (MeV/c^2)	0.853 ± 0.002	2.715 ± 0.005	5.147 ± 0.014	5.613 ± 0.046

From the two large-Q-value Λ_c^+ data samples measurements of the Λ_c^+ mass were obtained and that can be compared to the more precise measurements from the $\Lambda_c^+ \to \Lambda K^0_S K^+$ and $\Lambda_c^+ \to \Sigma^0 K^0_S K^+$ samples. To keep the systematic uncertainty low, only $\Lambda_c^+ \to pK^-\pi^+$ and $\Lambda_c^+ \to pK^0_S$ candidates with laboratory momentum above $3\,\mathrm{GeV}/c$ are used. The results are shown in Table III and are in good agreement with the main result, but have larger systematic uncertainties. In the same table also the corrected values for Λ and K^0_S are shown and they are in good agreement with the PDG. Since the Λ and K^0_S candidates are the same candidates used in the final Λ_c^+ sample, the agreement with the PDG mass values gives further confidence in the Λ_c^+ mass result.

TABLE III

Corrected values for the four decay modes used for cross-checks (the first error is statistical, the second systematic).

Parameter	$\Lambda \to p\pi^-$	$K^0_S \to \pi^+\pi^-$
Fitted mass (MeV/c^2)	1115.68± 0.01±0.04	497.56±0.04±0.26

Parameter	$\Lambda_c^+ \to pK^-\pi^+$	$\Lambda_c^+ \to pK^0_S$
Fitted mass (MeV/c^2)	2286.39± 0.02±0.45	2286.36±0.03±0.43

5. Ω_c^0 and Ξ_c^0 production and decay

Ω_c^0 production and decay[2] is studied using about 230 fb^{-1} of data collected by BaBar (on and off resonance), while the Ξ_c^0 [10] analysis is based on 116.1 fb^{-1} (on and off resonance). The Ω_c^0 is studied through the decay modes[3] $\Omega^-\pi^+$, $\Omega^-\pi^+\pi^-\pi^+$ and $\Xi^-K^-\pi^+\pi^+$ while the Ξ_c^0 is studied in the decays $\Xi_c^0 \to \Omega^- K^+$ and $\Xi_c^0 \to \Xi^-\pi^+$. The Ω^- (Ξ^-) is reconstructed in its ΛK^- ($\Lambda\pi^-$) final state. Candidates for Λ decays are reconstructed in their $p\pi^-$ final state. All hyperons in this analysis (Λ, Ξ^-, and Ω^-) are long-lived particles with a typical decay length of several cm in BaBar. Each hyperon is identified by reconstructing its decay vertex, which is required to be clearly displaced from that of the parent particle.

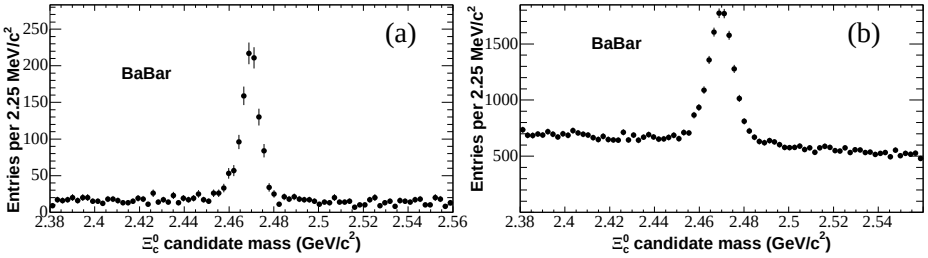

Fig. 3. Ξ_c^0 invariant mass distributions for (a) $\Omega^- K^+$ and (b) $\Xi^-\pi^+$.

The Ξ_c^0 invariant mass distributions are shown in Fig. 3 (a) and (b) for $\Omega^- K^+$ and $\Xi^-\pi^+$ combinations, respectively. To measure the ratio of branching fractions, the requirement that $p^* > 1.8\,\mathrm{GeV}/c$ is imposed on the Ξ_c^0 candidates, improving the signal purity. The efficiency is calculated from signal Monte Carlo events as a function of p^* and $\cos\theta^*$ for each of the decay modes. Including efficiency loss due to the Ω^- and Λ branching fractions, 25889 ± 516 events in the $\Xi^-\pi^+$ mode and 7615 ± 443 events in the $\Omega^- K^+$ mode are obtained. The ratio of branching fractions result:

$$\frac{\mathcal{B}(\Xi_c^0 \to \Omega^- K^+)}{\mathcal{B}(\Xi_c^0 \to \Xi^-\pi^+)} = 0.294 \pm 0.018(\mathrm{stat}) \pm 0.016(\mathrm{syst})\,,$$

where the first uncertainty is statistical, the second is systematic; this measurement is consistent with the prediction from the spectator quark model calculation (0.32) [11].

The Ω_c^0 invariant mass spectra are displayed in Figs. 4(a), (b) for the $\Omega^-\pi^+$ and $\Xi^-K^-\pi^+\pi^+$ modes. The results of the fits to the data, the selection efficiencies[4], and the χ^2 probability for each fit are summarized in Table IV. In addition, the significance $\mathcal{S}$ for the signal is included.

[2] The results on Ω_c^0 production and decay are preliminary.
[3] Simultaneous treatment of the charge conjugate mode is always implied.
[4] All selection efficiencies quoted are for Ω_c^0 decays with $p^* > 2.8\,\mathrm{GeV}/c^2$.

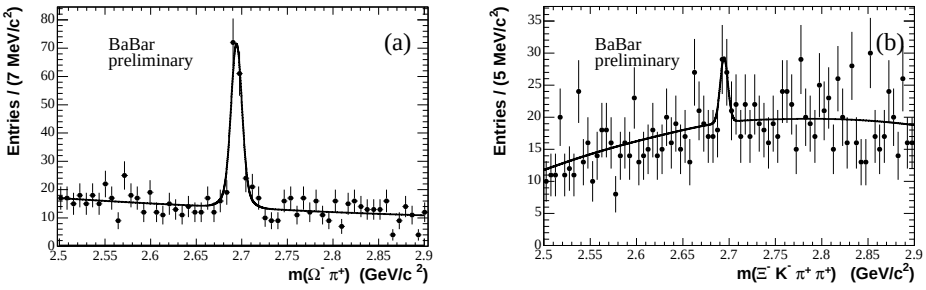

Fig. 4. Invariant mass spectra for Ω_c^0 decays into (a) $\Omega^-\pi^+$ and (b) $\Xi^-K^-\pi^+\pi^+$ final states with $p^* > 2.8\,\mathrm{GeV}/c$. The result of the fit is overlaid.

TABLE IV

Preliminary results from the fits to the invariant mass spectra in data. The yields (not corrected for efficiency) are given for each mode individually, as well as the selection efficiencies.

Decay mode	Signal yield	Efficiency (%)	prob(χ^2)	$\mathcal{S}$
$\Omega^-\pi^+$	138.5 ± 14.8	8.35 ± 0.07	0.54	17.8
$\Omega^-\pi^+\pi^-\pi^+$	11.8 ± 7.5	4.41 ± 0.09	0.73	2.4
$\Xi^-K^-\pi^+\pi^+$	29.9 ± 13.6	5.63 ± 0.10	0.85	3.4

To measure the ratio of branching fractions, the requirement that $p^* > 2.8\,\mathrm{GeV}/c$ is imposed on the Ω_c^0 candidates. The yields for Ω_c^0 signal events, extracted from the invariant mass spectra in the data and corrected for selection efficiency and acceptance effects. These are extracted from reconstructed signal Monte Carlo events that pass the same selection criteria as events in data. The efficiency corrected yields are then used to calculate the ratios of branching fractions relative to the $\Omega_c^0 \to \Omega^-\pi^+$ mode, yielding

$$\frac{\mathcal{B}(\Omega_c^0 \to \Omega^-\pi^+\pi^-\pi^+)}{\mathcal{B}(\Omega_c^0 \to \Omega^-\pi^+)} = 0.16 \pm 0.10(\mathrm{stat}) \pm 0.03(\mathrm{syst})\,,$$
$$\frac{\mathcal{B}(\Omega_c^0 \to \Xi^-K^-\pi^+\pi^+)}{\mathcal{B}(\Omega_c^0 \to \Omega^-\pi^+)} = 0.31 \pm 0.15(\mathrm{stat}) \pm 0.04(\mathrm{syst})\,.$$

Ξ_c^0 and Ω_c^0 production is studied by measuring the spectrum of the baryon momentum in the e^+e^- center-of-mass frame (p^*). A number of theoretical predictions of the rate of Ξ_c production in B decays have been made [12–15]. Insight into the contributing processes can be gained by studying the shape of the p^* spectrum. Evidence for Ξ_c^0 production in B decays

was presented previously by the CLEO Collaboration [16]; for the Ω_c^0 the first evidence of production in B decays is presented.

For the Ω_c^0 study, the $\Omega_c^0 \to \Omega^-\pi^+$ decay mode, which has the largest signal yield of all modes in this analysis, is used. The measured signal yields obtained from the combined on-peak and off peak data sets can be compared with those from the off-peak data set, displayed in Figs. 5(a) and (b), respectively. The dots represent the data and the error bars correspond to the statistical uncertainty only. The solid horizontal bars correspond to the predicted spectrum for Ω_c^0 production from $c\bar{c}$ continuum Monte Carlo; the thickness of the bars correspond to the statistical uncertainty. No correction for selection efficiency is applied to either distribution. The corresponding distribution from signal Monte Carlo is normalized such that its integral corresponds to that in data for $p^* > 2.5\,\mathrm{GeV}/c$ in Fig. 5(a), and for the full p^* range in Fig. 5(b).

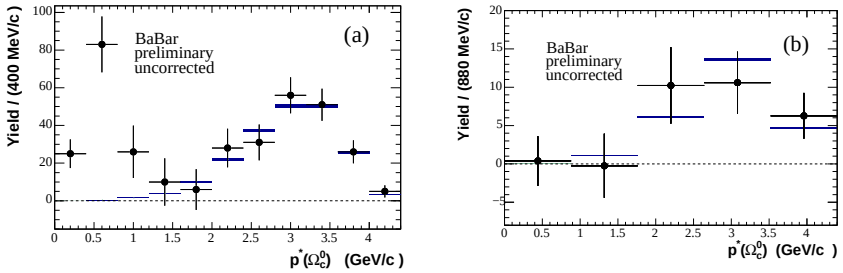

Fig. 5. The signal yield as a function of the p^* of Ω_c^0 candidates (a) from the combined on-peak and off-peak data sets and (b) from off-peak data only.

A clear two-peak structure is evident in the distribution from the combined on-peak and off-peak data sets. The peak at high p^* is consistent with Ω_c^0 production as predicted from continuum signal Monte Carlo and the off-peak data. The p^* spectra from data and Monte Carlo show good agreement within the experimental uncertainties in this region. The peak in the p^* region below $2.02\,\mathrm{GeV}/c$ provides clear first evidence for Ω_c^0 production from B decays. This interpretation is substantiated by the absence of the corresponding peak in the spectrum extracted from off-peak data only, taken below the $B\bar{B}$ threshold.

The double-peak structure seen in the Ω_c^0 p^* spectrum is also visible in the Ξ_c^0 sample, the peak at lower p^* is due to Ξ_c^0 production in B meson decays and the peak at higher p^* is due to Ξ_c^0 production from the $c\overline{c}$ continuum. This is evident from Fig. 6, where the p^* spectra for the on-resonance and off-resonance data are shown separately (with the off-resonance spectrum scaled to the on-resonance integrated luminosity and corrected for the change in $c\overline{c}$ cross-section). The $c\overline{c}$ peak is present in both samples, but

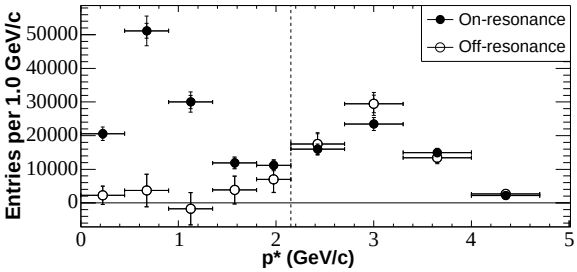

Fig. 6. The p^* spectrum measurements, the on-resonance and off-resonance data samples are shown together, with the off-resonance normalization scaled to account for the difference in integrated luminosity and cross-section. The vertical line at $2.15\,\mathrm{GeV}/c$ shows the kinematic cutoff for Ξ_c^0 produced in B decays at BaBar.

the $B\overline{B}$ peak is only present in the on-resonance sample. Assuming baryon number conservation, the kinematic limit for Ξ_c^0 produced in the decays of B mesons at BaBar is $p^* = 2.135\,\mathrm{GeV}/c$. To obtain the yield of Ξ_c^0 produced in B decays, the on-resonance and scaled off-resonance samples for $p^* \leq 2.15$ GeV/c are compared; this is scaled by the number of B mesons in the data sample to obtain

$$\mathcal{B}(B \to \Xi_c^0 X) \times \mathcal{B}(\Xi_c^0 \to \Xi^- \pi^+) = (2.11 \pm 0.19 \pm 0.25) \times 10^{-4}\,.$$

The yield of Ξ_c^0 produced in $c\overline{c}$ events at an energy of $10.58\,\mathrm{GeV}$ is calculated from the scaled off-resonance data set (for $p^* \leq 2.15\,\mathrm{GeV}/c$) and the on-resonance data set (for $p^* > 2.15\,\mathrm{GeV}/c$). The yield is then divided by the integrated luminosity to obtain the cross-section from the continuum

$$\sigma(e^+e^- \to \Xi_c^0 X) \times \mathcal{B}(\Xi_c^0 \to \Xi^- \pi^+) = (388 \pm 39 \pm 41)\,\mathrm{fb}\,,$$

where both Ξ_c^0 and $\overline{\Xi}_c^0$ are included in the cross-section. The effect of initial state radiation is not isolated.

6. Conclusions

The very high statistics available at B-factories in a clean environment, while enhances the discovery capabilities of new resonances ($Y(4260)$), it gives also the possibility to greatly improve our knowledge, by making more precise measurements of the masses of known states (as is the case of Λ_c^+) or decay branching ratios and production mechanisms (Ξ_c^0 and Ω_c^0) giving theory an hint on the models underlying these states. In the next years the available statistics will double, giving opportunities to better constrain our knowledge from an experimental point of view.

REFERENCES

[1] B. Aubert *et al.*, *Nucl. Instrum. Methods* **A479**, 1 (2002).

[2] BELLE Collaboration, S.K. Choi *et al.*, *Phys. Rev. Lett.* **91**, 262001 (2003).

[3] M. Benayoun *et al.*, *Mod. Phys. Lett.* **A14**, 2605 (1999).

[4] BaBar Collaboration, B. Aubert *et al.*, *Phys. Rev.* **D71**, 052001 (2005).

[5] B. Aubert *et al.*, *Phys. Rev. Lett.* **95**, 142001 (2005).

[6] X.C. Lou, *Int. J. Mod. Phys.* **16**, No. supp01B, 486 (2001).

[7] S. Eidelman *et al.*, Particle Data Group, *Phys. Lett.* **B592**, 1 (2004).

[8] B. Aubert *et al.*, submitted to *Phys. Rev.* **D**, `hep-ex/0507009`.

[9] L. Lyons, D. Gibaut, P. Clifford, *Nucl. Instrum. Methods* **A270**, 110 (1988).

[10] B. Aubert *et al.*, *Phys. Rev. Lett.* **95**, 142003 (2005).

[11] J.G. Körner, M. Krämer, *Z. Phys.* **C55**, 659 (1992).

[12] P. Ball, H.G. Dosch, *Z. Phys.* **C51**, 445 (1991).

[13] V.L. Chernyak, I.R. Zhitnitsky, *Nucl. Phys.* **B345**, 137 (1990).

[14] S.M. Sheikholeslami, M.P. Khanna, *Phys. Rev.* **D44**, 770 (1991).

[15] I. Dunietz, P.S. Cooper, A.F. Falk, M.B. Wise, *Phys. Rev. Lett.* **73**, 1075 (1994).

[16] CLEO Collaboration, B. Barish *et al.*, *Phys. Rev. Lett.* **79**, 3599 (1997).